

LARGE ARRAYS OF INKJET-PRINTED MEMS MICROBRIDGES ON FOIL

Francisco Molina-Lopez, Danick Briand, and Nico F. de Rooij

Ecole Polytechnique Fédérale de Lausanne (EPFL), Neuchâtel, SWITZERLAND

ABSTRACT

This work describes the fabrication process of an array of printed MEMS microbridges on polymeric foil, performed in only four easy steps. Each functional material was deposited exclusively by inkjet-printing technique, compatible with large-area fabrication. The array occupies an area of 2 mm x 2 mm and consists of 80 individual microbridges of 120 μm x 80 μm size each. When connecting all the bridges in parallel, the array displays a total capacitance value of 1.5 pF. The potential of the fabricated array has been demonstrated by employing it as a swelling-based capacitive humidity sensor where the polymeric substrate acts directly as the sensing layer.

INTRODUCTION

MEMS are gaining interest in the field of large-area systems due to the possibility to employ them in many new applications. For example, the fabrication of a “smart MEMS sheet” for the displacement of small objects on a flexible foil has been presented by Ataka *et al.* in 2013 [1]. MEMS are typically fabricated using clean room processes which limit their realization on a large-area and contribute to the increase of production costs. The application of printing fabrication techniques to MEMS production process would make it possible to combine the typical advantages of printing (such as low fabrication costs and compatibility with a broad range of materials and substrates) with the functionalities of MEMS. Among the different printing techniques, inkjet stands out for its simplicity and versatility due to its non-contact and digital character. A work combining inkjet-printed organic transistors with polymeric actuators on a large-area was reported in [2] for the fabrication of flexible ultrasonic systems. In that case, the actuators had sizes in the millimeter range and were not fabricated by printing methods. Nonetheless, inkjet-printed MEMS have been recently reported in [3], where the authors described the fabrication of cantilever-based switches through a relatively complex process involving also spin coating and the definition of via-holes.

In this work, we benefit from the advantages of inkjet-printing to develop arrays of fully printed MEMS microbridges on polymeric foil through four simple steps, all of them compatible with large-area fabrication. The microbridges have been characterized by electrostatic actuation and then, their operation as capacitive relative humidity sensors has been demonstrated. Fully inkjet-printed capacitive humidity sensors have already been fabricated on polymeric foil as reported in [4, 5]. Their operation was based on the changes in the permittivity of a sensing layer in the presence of moisture. Here, we propose a new working principle for gas sensing based on the swelling of a polymeric substrate which acts as a sensing

layer. The application of the device as a capacitive sensor became possible owing to the high capacitance value provided by many microbridges connected in parallel. The microbridges array could also be adapted for detection of more specific gases by functionalizing the substrate, passivating it against permeation of moisture (or other gases), or inkjet-printing another custom-made swelling sensing layer onto the bridge. When compared to a membrane-like device providing an equivalent capacitance value, this device presents advantages in terms of fabrication simplicity, mechanical robustness and little sensitivity to accelerations due to the small mass of every independent microbridge. Finally, the reported device could be turned into an array of micro-switches or micro-actuators by tailoring the geometry of the microbridges. This work foresees the potential of low-cost and large-area printed MEMS structures for sensing and actuating applications.

DESIGN

The presented device consisted of an array of 80 microbridges like the one sketched in Figure 1 that could function separately or altogether. Each bridge was designed to be formed by a 200 nm-thin, 65 μm -wide silver bottom electrode; and a thicker ($\sim 2 \mu\text{m}$) 80 μm -wide suspended silver top electrode / microbridge. The microbridge was fabricated with the help of a sacrificial layer of photoresist placed in between the two electrodes. The thickness of the sacrificial layer was $\sim 5 \mu\text{m}$ and corresponded with the height of the microbridge. The expected capacitance value of every single bridge was of ~ 20 fF.

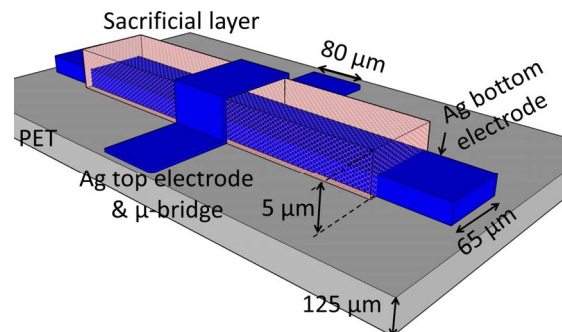


Figure 1: Sketch of the microbridge before being released.

In the array (see Figure 3), the bridges were arranged in 10 columns separated by a distance of 200 μm . Each column was composed by 8 rows of microbridges placed in line and separated by a distance of 240 μm . The bottom electrode was a continuous layer shared by the 10 microbridges in the same row. In order to reach a capacitance value easy to read with standard laboratory instruments, the 80 bridges in the device were connected in parallel. All the bottom electrodes were connected together

by large pads placed at both sides of the array. Similarly, all the bridges were contacted by pads placed above and below the array. The size of the pads was 1 mm x 1 mm. The total expected capacitance was of 1.5 pF.

FABRICATION

Materials and Methods

All the chemicals employed during the fabrication of the MEMS array were purchased from *Sigma-Aldrich* and used as they were unless otherwise stated. The device was fabricated on a substrate made of 125 μm -thick polyethylene terephthalate (PET) *Melinex® ST506* from *Dupont Teijim Films*. Both bottom and top electrode (the bridge itself) were composed of silver-nanoparticles ink (*SuntTronic Jet EMD506* from *SunChemical*) with 20% solid content. The sacrificial layer was commercial photoresist *Microposit® 1813®* from *Shipley* diluted 90:10 (% weight) with propylene glycol monomethyl ether acetate (PGMEA) to make it inkjet-printable by the utilized printer *Dimatix Fujifilm DMP-2800™* with 10 pL drop volume cartridges.

Process Flow

Figure 2 shows the steps of the fabrication process, along with an optical picture of the device at the end of every step. Prior to the printing of the bottom electrode, the substrate was cleaned by successive immersion in acetone, isopropanol (both VLSI grade) and deionized water baths for 10 minutes. After drying with nitrogen, the substrate was subjected to a thermal treatment for 30 minutes at 140 °C for dehydration and thermal stabilization. Then, we treated the substrate with low frequency (13.56 MHz) oxygen plasma for 35 seconds at 50 W to increase the substrate surface wettability. An undesired side effect of the oxygen plasma treatment was a large spreading of the ink on the substrate, resulting in very wide printed lines. This effect was considerably reduced while maintaining good wettability by heating up again the substrate in the oven for 5 minutes at 120 °C. The bottom electrode was formed by inkjet-printing two consecutive layers of silver ink with a drop-to-drop separation of 40 μm (Figure 2 (a)). Following, the silver was sintered at 140°C for 30 minutes in a convection oven. In the second step, two layers of the diluted photoresist were also inkjet-printed, with a drop-to-drop spacing of 20 μm , on top of the bottom electrode to act as sacrificial layer (Figure 2(b)). Special care was taken during the alignment of the resist on the bottom electrode to ensure its total coverage and to avoid future short-circuits between the top and the bottom electrodes. After the resist was annealed on a hot plate at 115 °C for 10 minutes, the same silver ink was inkjet-printed on it to form the top electrode / microbridge. The annealing of the resist was needed to render it chemically resistant to the solvent of the silver ink. Nine consecutive layers with a drop-to-drop space of 20 μm were printed to form the microbridge, which was afterwards sintered on a hot plate at 115 °C for 30 minutes (Figure 2 (c)). Although this sintering temperature

was rather mild and led probably to bridges with poor mechanical properties, we could not increase it since we observed difficulties to dissolve the resist when it underwent temperatures higher than 115 °C. At this point, optional electrodeposition of Ni has been also demonstrated to thicken the bridge if necessary (Figure 2 (d)). Finally, the sacrificial layer was removed by dissolving it in acetone (Figure 2 (e)). Stiction problems were avoided by performing freeze-drying process: the acetone under the bridge was successively replaced by isopropanol and finally by cyclohexane (HPLC grade), which was frozen on a Peltier element (freezing point 6.47 °C) and sublimated under nitrogen atmosphere.

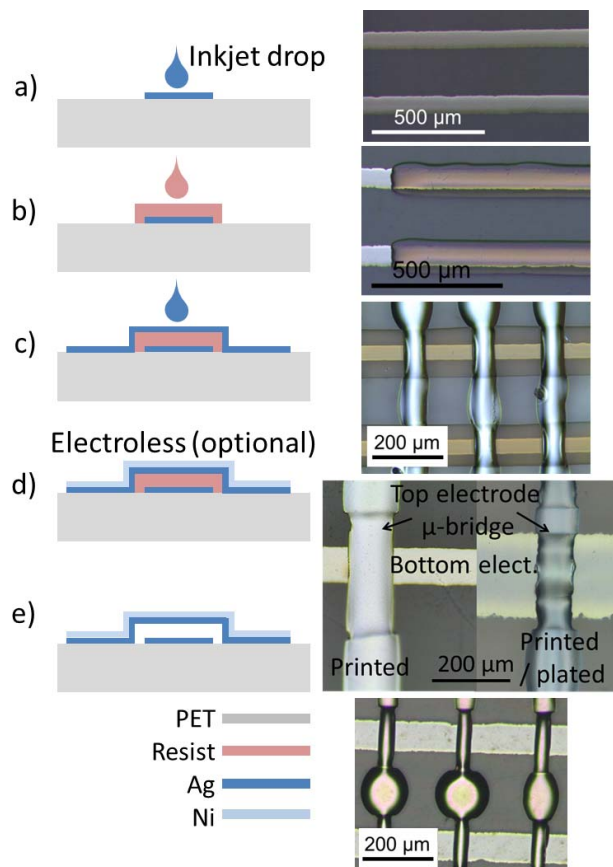


Figure 2: Sketch (left) and optical images (right) of every step of the microbridges fabrication process.

RESULTS

Fabrication of Arrays of MEMS Microbridges

Several arrays of MEMS microbridges were successfully inkjet-printed on PET foil. Figure 3 contains optical images of the arrays where the different parts have been labeled. The figure also includes a scanning electronic microscope (SEM) image of the array and a 3D image, obtained with a white light interferometer. The accumulation of ink between the bridges during the printing process formed pillars-like structures which were not found to be unfavorable for the proper operation of the device.

The use of inkjet-printing to fabricate MEMS makes it

easy to control the height of the bridge as well as its thickness by choosing the number of printed layers. Figure 4 depicts the relationship between the thickness and the number of printed layers for the sacrificial photoresist layer and the silver microbridge. The final selected values, $\sim 5 \mu\text{m}$ thick photoresist and $\sim 2 \mu\text{m}$ thick top electrodes, were chosen based on empirical observations, seeking to maximize the fabrication yield. Although Figure 4 (bottom) indicates that 6 printed layers were sufficient to print $\sim 2 \mu\text{m}$ thick top electrode, the flow of the ink toward the pillars made necessary to print 9 layers as indicated in the process flow above. The bridges have a typical height of $\sim 2.5 \mu\text{m}$ (smaller than the thickness of the sacrificial layer since the bridges tend to move down after being released), a length of $120 \mu\text{m}$ and a width ranging from 60 to $80 \mu\text{m}$. The bottom electrode width resulted in $65 \mu\text{m}$.

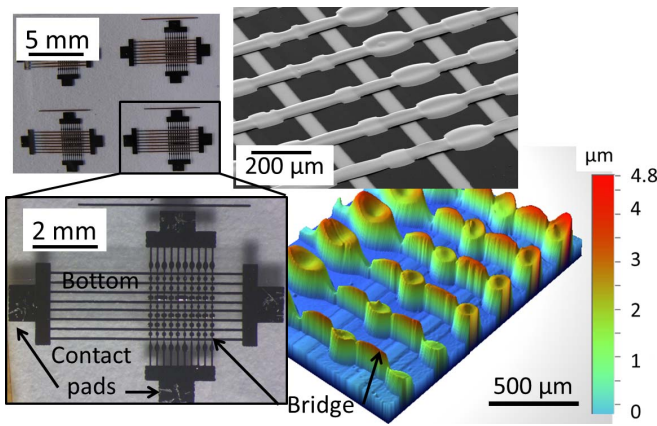


Figure 3: Optical image and magnification view of the array of microbridges (left). SEM image of the array (top right) and white light interferometer image of the same array (bottom right).

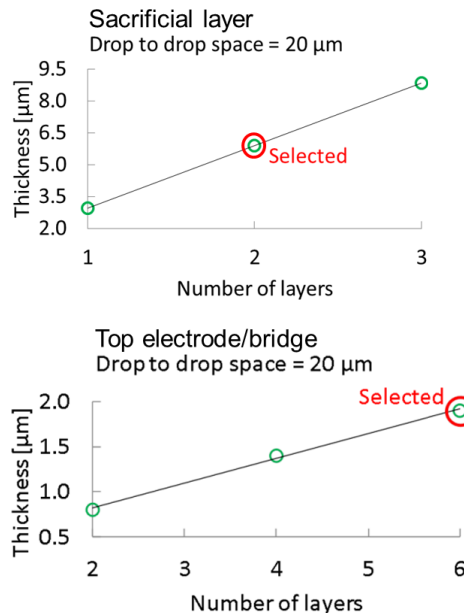


Figure 4: Thickness of the inkjet-printed sacrificial layer (top) and bridge (bottom) versus number of printed layers.

Electrostatic Actuation

In order to confirm the operation of the devices as suspended structures, they were electrostatically actuated by applying a voltage between their bottom and top electrode, while measuring at the same time the deflection of the top electrode. Figure 5 shows the deflection of a single device with applied voltage, measured with a white light interferometer. The distance between the top and the base of the released microbridge is $1.6 \mu\text{m}$ in the absence of any applied voltage.

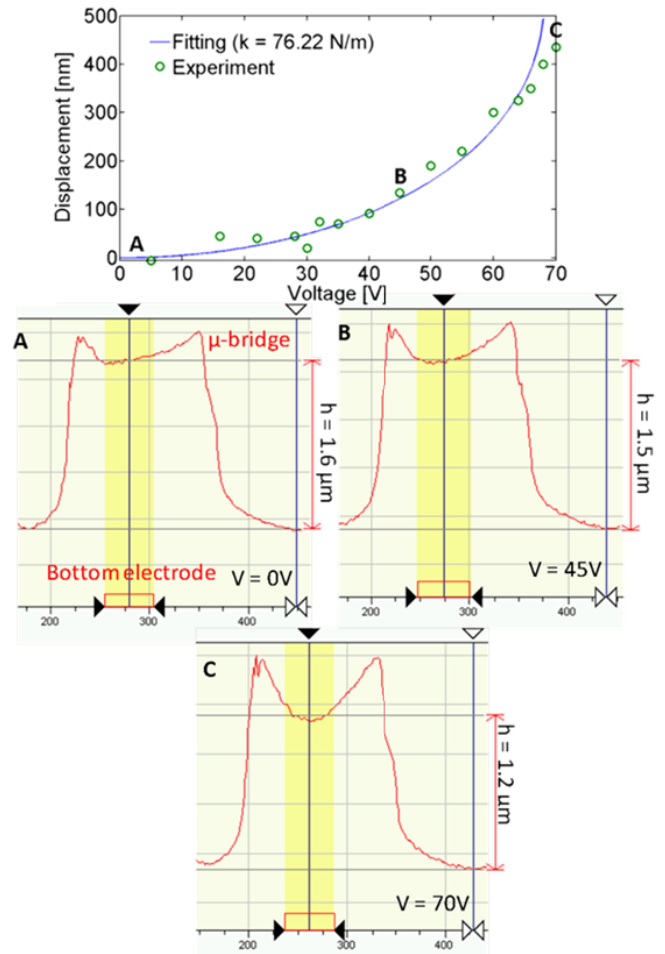


Figure 5: Microbridge displacement versus applied voltage: experimental points and fitting curve with a deduced effective spring constant (top). Microbridge profile measured at different voltages (bottom).

A mathematical fitting to the experimental values has been performed (Figure 5 (top)) using the parallel-plate model which states that in static mode, the mechanical force on the bridge F_M is equal to the electrostatic one F_E :

$$F_M = k d = F_E = \frac{1}{2} C V^2 / (g - d) \quad (1)$$

where d is the deflection of the bridge, C the parallel plate capacitance formed between bottom and top plates, V the applied voltage and g the original gap in between the plates.

The effective spring constant for the shown bridge resulted in $k = 76 \pm 4$ N/m. This constant can be modified by changing the material of the bridge, its sintering conditions or the bridge geometry; making possible to adjust the stiffness of the bridge to the required application.

Application as Humidity Sensors

Since the substrate of the devices is a polymer, it swells upon gas absorption. We could then assume that the substrate bends and the bridges buckle up increasing the distance between the bottom and the top electrode. The capacitance value of the array should therefore decrease accordingly. In this way, the device can be used as a gas sensor. The results shown in Figure 6 (where $C' < C$) seem to confirm our assumptions. The tests were carried out for relative humidity for the sake of simplicity but the principle applies to every gas in general. The device was introduced in a climatic chamber and subjected to different steps of relative humidity (25%, 45% and 65% r.h.) while keeping the temperature fixed at 30°C. After letting the sensor to stabilize for 30 minutes, the capacitance value was registered at 100 kHz for every step using an LCR-meter. The device was tested for two downsweep and one upsweep cycles and it displayed a linear behavior with a coefficient $R^2 = 0.9757$ and a precision of 4.3% r.h. The sensitivity was -1.92 ± 0.14 fF / 1% r.h. As opposed to the most part of polymeric printed capacitive gas sensors already present in the literature (see as an example [4, 5]), the microbridge-based sensor does not rely on variations in electrical permittivity, but on mechanical swelling. Hence, they are expected to be more sensitive to large molecules, such as volatile organic compounds (VOCs), than to small water molecules, despite the high permittivity of the latter. These bridges-based sensors are thus a perfect complement to the ones already reported.

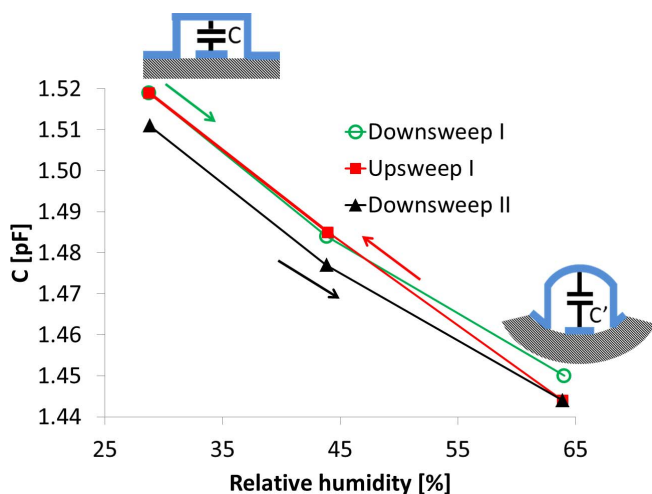


Figure 6: Capacitance value versus relative humidity displayed by the MEMS array operating as a humidity sensor, along with a sketch of the expected bridge behavior.

In order to expand the functionality of the sensor towards more specific analytes, it would be also possible to

coat the bridge with a customized sensing layer. This would induce stress on the bridge itself too. Non-contact printing methods such as inkjet or laser induced forward transfer (LIFT) would be suitable methods for such purpose. Alternatively, the substrate could be functionalized or passivated at the same time to tailor the selectivity of the sensor.

CONCLUSIONS

Large arrays of fully inkjet-printed MEMS silver microbridges have been fabricated on PET foil through only four process steps. After confirming the electrostatic actuation of the bridges, we demonstrated the possibility of interconnecting the 80 bridges of the array in parallel to provide readable capacitance values of 1.5 pF. The potential of the device as a capacitive humidity sensor was then assessed by directly utilizing the polymeric substrate as a swelling sensing layer. By coating the bridges with a customized sensing layer or by functionalizing / passivating the substrate, the operation of the sensor could be expanded to detection of others analytes. For future improvements, a theoretical model should be elaborated to predict the sensor response to gases. Finally, by optimizing the pull-in voltage of every microbridge, the device could work as an array of MEMS switches.

ACKNOWLEDGEMENTS

EU FP7 Project FlexSmell, Marie-Curie ITN. Grant 238454. We also acknowledge the SNF R'Equip program.

REFERENCES

- [1] M. Ataka, *et al.*, "Micro Actuator Array on a Flexible Sheet – Smart MEMS Sheet", in *Proc. MEMS 2013*, Taipei, January 20-24, 2013, pp. 536-539.
- [2] Y. Kato *et al.*, "Large-area Flexible Ultrasonic Imaging System with an Organic Transistor Active Matrix", *IEEE Transaction on electron devices*, vol. 57 (5), pp. 995-1002, 2010.
- [3] E.S. Park *et al.*, *Nanoletters*, "A New Switching Device for Printed Electronics: Inkjet-printed Microelectromechanical Relay", vol. 13, pp. 5355-5360, 2013.
- [4] F. Molina-Lopez *et al.*, "Large-area Compatible Fabrication and Encapsulation of Inkjet-printed Humidity Sensors on Flexible Foils with Integrated Thermal Compensation", *J. Micromech. Microeng.*, vol. 23, pp. 025012, 2013.
- [5] F. Molina-Lopez *et al.*, "Decreasing the Size of Printed Comb Electrodes by the Introduction of a Dielectric Interlayer for Capacitive Gas Sensors on Polymeric Foil: Modeling and Fabrication", *Sens. Act. B: Chem.*, vol. 189, pp. 89-96, 2013.

CONTACT

*F. Molina-Lopez, tel: +41-21-695-4434; francisco.molinalopez@epfl.ch